International Journal of Health Sciences

Available online at www.sciencescholar.us
Vol. 6 No. 2, August 2022, pages: 880-897
e-ISSN: 2550-696X, p-ISSN: 2550-6978
https://doi.org/10.53730/ijhs.v6n2.8735

Malaria Diagnosis Using Microscopic Imaging

Mosam K. Sangole [a], **Sanjay T. Gandhe** [b]

Manuscript submitted: 20 January 2022, Manuscript revised: 19 April 2022, Accepted for publication: 30 May 2022

Corresponding Author [a]

Keywords

cubic SVM;
malaria parasite;
microscopy blood smear;
Otsu;
SAMF;

Abstract

Malaria, a dangerous disease caused by Plasmodium, which is spread by being bitten by infected mosquitoes (Female Anopheles). It is crucial to diagnose malaria pathogens quickly and accurately at the right time. Traditional microscopy is commonly used in developing countries to diagnose malaria parasites, where pathologists examine the slide under a light microscope. However, in the case of traditional microscopy, requires more time and careful attention. Here, we have proposed a method to diagnose malaria based on computer vision. As a pre-processing stage, SAMF (Systematically Applied Mean Filter) algorithm is proposed that removes impulse noise from the corrupted malaria-infected images. Otsu method is used to obtain the binary version of images for cropping blood cells from complete image. 17 texture and color features were extracted from these cropped cells and these features were used to train Cubic SVM (Support Vector Machine) classifier. Hence a precise malaria diagnosis system was developed for detecting Plasmodium parasites, identifying their life stages and species using images of thin blood smears. A total of 348 images from CDC (Centre for Disease Control and Prevention) database were used to train and test the performance of the system.

Contents

Abstract 880
1 Introduction 881
2 Materials and Methods 885
3 Results and Discussions 888
4 Conclusion 893
Acknowledgments 893
References 894
Biography of Authors 897

[a] Sandip Institute of Technology and Research Center, Nashik, India
[b] Sandip Institute of Technology and Research Center, Nashik, India

1 Introduction

The most common type of cells in human body is erythrocytes, which is supply oxygen to all body tissues. Abnormal erythrocytes can change their physical properties or shorten their lifespan, and may also lead to malaria. As per the "World Malaria Report 2019" issued by the “W.H.O.”, an estimated 200 million people were infected and 400,000 died (Gonz´alez et al., 2015). Malaria is produced by a parasite in the blood or liver. Different types of Plasmodium parasites that cause malaria in humans are Plasmodium falciparum, Plasmodium ovale, Plasmodium vivax and Plasmodium malariae. These Plasmodium species infect erythrocytes and go through different life phases; early trophozoites, mature trophozoites, gametocytes and schizoites. Fig.1 shows some sample images of different species along with different stages of Plasmodium.

Appearances of malaria parasites at different stages and species are described in table 1, which were observed under a microscope (Lee & Chen, 2014). Red blood cells infected by parasites do not swell, and usually more than one type of parasite can be seen in the cells. Microscopic diagnosis has several advantages: it can distinguish species, can check the stage of parasites, and quantify parasitemia (Lee & Chen, 2014). In addition, it is highly sensitive and specific for detecting Plasmodium species at various stages. The classification of parasites and their types is very useful for studying the characteristics of malaria, as well as for prevention and diagnosis. However, this is a tedious and laborious task, and the knowledge and expertise of trained professionals play a big role in the precision of diagnosis (Elsalamony, 2016). Therefore, it is very vital to design a computerized automatic system to detect the type of parasite and phases. Segmentation of the infected erythrocytes and then removal of parasites (type and stage) from infected erythrocytes is required for the development of a computerized disease detection system.

Stages Species	Ring Stage	Trophozoite	Schizont	Gametocyte
P.Falciparum	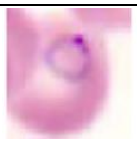		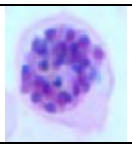	
P.Vivax				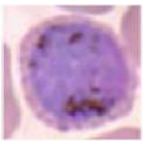
P.Malariae		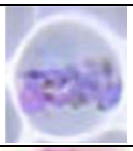		
P.Oval			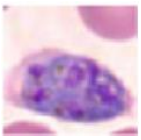	

Figure 1. Four Plasmodium species during four phases of development (Fatima & Farid, 2020)

Table 1
Different stages of the malaria parasite exhibiting different morphological characteristics

Species Parameters	P.Falciparum	P.Vivax	P.Malariae	P.Oval
Red cell inflammation	No	Yes	No	Oval formed
Speckling	No	Schueffner	No	Schueffner
Circle form	Small	Large	Small	Large
Tropozoite	Not seen	Amoeboid	Band form	Oval
Schizont	Not seen	Large	Small	Small
Number of merozoites	16 to 24	14 to 20	8 to 10	6 to 12
Stain particle	Grainy grouped	Fine distributed	Grainy ample	Fine
Gametocyte	Crescent shaped	Round to oval large	Round to oval small	Round to oval small

Literature review

There have been several feasibility studies on automating traditional microscopes, and this section reviews some of them. The importance of many features in the classification of erythrocytes infected with malaria was indicated by (Devi et al., 2018). To categorize the erythrocytes, a classification model based on ANN-GA was developed. Various classification algorithms such as Support vector machine (SVM), K-nearest neighbor (KNN), and Naive Bayes method are evaluated using 6 sets of features (morphological features, texture features, and intensity features). From experimental results it is proved that the f6 feature set (combination of morphological attributes, texture attributes and intensity, classified by ANOVA) is better than other feature sets. In addition, ANNGA of feature set f6 is used to classify erythrocytes.

Fatima & Farid (2020), proposed a method for removing noise and improving image quality by employing bilateral filtering. Malaria parasites are detected in individual cells using morphological imaging methods and adaptive thresholds. Compared with competing methods, it achieves a recognition accuracy of over 91%. The Scale Invariant Feature Transform (SIFT) was used to extract features, and the Support Vector Machine (SVM) was used to classify them, by (Gezahegn et al., 2018). The overall performances of the investigation are, 76.67% specificity, 80% sensitivity and 78.89% accuracy.

Somasekar & Reddy (2015), suggested a technique for edge segmentation of malaria cells on blood images. The author compares the suggested method with seven other customary edge segmentation approaches and concludes that the suggested method is effective in segmenting erythrocytes which are infected by parasite. The segmentation along the edge of the erythrocytes infected with the malaria parasite was developed using microscopic images to assist the detection procedure (Okhabska et al., 2022). Color space conversion and gamma alignment can decrease color effects and correct variances in image brightness. Infected red blood cells extracted with Fuzzy C means clustering were used for further processing. The suggested execution time is longer than traditional edge segmentation methods.

In paper Mas et al. (2015), suggested a new image processing technique depending on locating cell movement and checking whether this movement is spatially dependent. The suggested theory depends on the analysis of the time variation of each pixel. This cell-to-cell activity occurred, indicating the presence of Plasmodium in the cell.

In paper Arco et al. (2015), a unique approach to automatically compute malaria parasites is suggested and assessed, with the use of a database which includes 475 photographs with various concentrations of malaria parasitic cells. This approach will examine information with the aid of utilizing typical procedures of image processing including histogram equalization, thresholding, morphological operations and connected component analysis for parasite concentration approximation.

In the literature Tomari et al. (2014), first extracts the red blood cell area from the background, uses the global threshold technique, and applies it to the color image of the green channel. Then uses the morphology filter and the marking of the connected components to remove the noise and holes from erythrocytes. These are extracted based on their geometric characteristics. Finally, an artificial neural network (ANN) classification algorithm is applied to classify erythrocytes as normal or abnormal. In detecting and counting the number of cells in the overlapping area, the suggested technique is unreliable.

In Das (2013), erythrocytes were segmented by marker-controlled watershed transformation, and then a total of 96 features were extracted, which describe the shape, size, and texture of erythrocytes related to infected and uninfected cells. As a feature selection and classification stage, Bayesian learning and support vector machine (SVM) were used. Other Plasmodium species, such as Plasmodium ovale and Plasmodium malariae, are not classified.

Tek et al. (2009), suggested a new parasite finding algorithm based on KNN RL1 distance classifier, which has some general descriptors. The author also suggested and compared three different classification algorithms which are used to identify different species and life cycles, and concluded that an ANN classifier with 20 categories can identify all three. In this work, the author used a limited set of data.

Sio et al. (2007), developed MalariaCount software, which can automatically generate parasitemia based on Giemsa-stained blood smear images. The stability and potential use of MalariaCount was verified in normal and drug-treated artificially inseminated cultures of P.falciparum. This work provides inaccurate parasitemia results for blood smears containing poorly colored, overlapping blood cells.

In Fatima & Farid (2020), depending on the use of circular Hough transform (CHT), watershed tools and morphology and neural networks to detect their shapes, the author proposed a method to identify healthy and unhealthy erythrocytes (elliptic cytosis, microcells, Sickle cell and shapeless cells).

Lee & Chen (2014), uses individual cell images extracted from blood smear microscopic images to classify red blood cells. They divided the entire collection of elements into two groups according to their characteristics: shapes and textures. They are used to process individual feature groups. Hybrid neural network architecture, including parallel and cascaded topologies, is used to classify red blood cells.

Rakshit & Bhowmik (2013), introduced the use of various instruments and imaging methods to correctly identify abnormalities in normal red blood cell parameters in anemia blood samples. Pre-processing is done using Weiner filter and the edges of the corpuscles are found using Sobel Edge detection method. Then, using the characteristics of the area, develop metrics to determine abnormal body shape to diagnose disease.

Khashman (2008), introduced an intelligent system that can simulate human visual inspection and the classification of three types of blood cells. The proposed system consists of two stages: the image pre-processing stage, in which the global average is used to extract the characteristics of blood cells, and the arbitration of the neural network i.e., the stage of training first and then classification. It is rotation invariant. Using a faster system can further reduce the time required. Further work includes expanding the blood cell database.

An automated malaria parasite and infected erythrocytes segmentation (MPIE) is presented in (Tsai, 2015). MPIE consists of 3 stages: pre-treatment (mean filtration and gamma equalization), object extraction (Sobel operation), detection and segmentation of infected RBCs and parasites. If the overlapped RBCs are classified as a region on the blood smear image, the MPIE method cannot give good results in separating the overlapped red blood cells.

Hung et al. (2015), developed a MP detector to accurately separate infected red blood cells and parasites from smear images. Investigational outcomes illustrate that the MP detector is superior to Malaria-Count in segmenting infected red blood cells and parasites. The weighted Sobel operation can offer sharper and finer object outlines during process of segmentation. However, if the overlapping RBCs are grouped in the same image area and the overlapping boundary is very blurred, the MP detector cannot separate them well.

Srivastava et al. (2015), develops SightDxP1 device which diagnose malaria and report parasitemia with only two species: P.vivax and P.falciparum. It consider P.ovale and P.falciparum species under P.vivax species.

Ghosh et al. (2017), uses a set of 4 related attributes of digital images to recognize different areas in the image. The various attributes of the recognition area are utilized to quantify erythrocytes (healthy and diseased) existing in the image. Regardless of the stage and species classification, red blood cell problems and overlapping red blood cells are partially visible.

The algorithm proposed in Delahunt et al. (2015), distinguishes hemozoin from non-haemozoin objects in the dark field (DF) of the image. Hemozoin was not detected in the parasites of the ring phase for less than 6 hours.

In the hemozoin is significantly different from the hemoglobin in the thin, unstained blood smear on the slide, which reduces the time required to stain the malaria sample. The spectral image was taken by means of a single LED lightened microscope equipped with a CMOS camera. The red blood cells were successfully divided using PCA.

Buggenthin et al. (2013), proposed a fully automated imaging pipeline that enables reliable but time-saving segmentation and analysis of ellipsoidal cells using high-throughput bright field microscopes. The process consists of two stages: (i) Image acquisition is accustomed to achieve the best quality of image in bright field for automatic processing. (ii) The combination of high-performance image processing algorithms reliably recognizes individual cells in each image. The proposed procedure does not support large-scale cell division.

In an automatic technique for detecting and classifying the species of malaria parasites in thick blood smears was introduced. The technique depends on digital image analysis and includes a motor-powered stage unit. The parasite species can be accurately classified as Pf or Pv using this analysis program, which is based on the chromatin size distribution. The image analysis unit comprises of 5 levels: image acquisition, pre-processing, image segmentation, feature extraction (chromatin size) and classification.

The diagnostic procedure in (Purwar, 2011) is divided into 2 parts; listing and identification. The image-based technology described here is intended to automate the process of recording and identification, the main advantage is to allow uncontrolled diagnosis and high sensitivity, thereby reducing false negatives, and if the platelet count is high, it will lead to incorrect counts of infected red blood cells.

Zuluaga et al. (2010), compared different haematology analyzer for malaria diagnosis such as Cell Dyn, Coulter Analyzer and XE – 2100. Author focuses to develop new haematology analyzer which are simple, robust and inexpensive.

The article summarizes and criticizes the research of computer vision and image analysis for the automatic detection of malaria in thin blood smears, providing its essential supporting functions. Ross et al. (2006), developed a method for detecting Plasmodium in liquid blood smears and identifying malaria species. Morphological and an innovative method (particle size measurement) of selecting a threshold is used to identify erythrocytes and any parasites that may be present. The proposed method fails the detection of mixed infections.

Chen et al. (2014), developed an automated technique for segmentation and classification of abnormal RBCs in blood smears of hemolytic anemia. First, a process based on 8 linked chain codes is used to separate the overlapping RBCs in the blood smear. Second, it detects normal and abnormal red blood cells using directional information from chain codes. Finally, hemolytic anemia is divided into 4 subtypes (hereditary elliptocytosis, sickle cell anemia, thalassemia, and glucose 6-phosphate dehydrogenase), including three new features, including different chain codes value, red blood cell irregularity and variability in eight directions.

Prasad et al. (2012), developed a assessment support system for diagnosing malaria by analyzing color images. The algorithm identifies suspicious areas and identifies parasites in images from all the observations. The partial images demonstrating all the parasites are combined into a combined image, which can be sent through a communication link to achieve inaccessible skilled opinions for precise detection and cure.

Banoth et al. (2016), advised a new application of high-throughput microfluidic microscopy to distinguish a source sample detector method based on light absorbance for the analysis of high-throughput single cells. The technology can be used to examine the chemical structure and morphological properties of RBCs at the same time.

It is proposed by the Eluru et al. (2015), a high-throughput method (800 cells/s) for determining cell deformation based on the single cell. The method includes acquiring images of the cells from the flow deformed in the guidance of the shear gradient produced by fluid rolling from microfluidic channels. The deformation index of such cells might be calculated by executing morphological procedures on these images.

Moon et al. (2013), used malaria-infected red blood cells to identify them by sidewise shear interferometry and statistical sampling. Disposable glass plates were used to obtain a shearing interferogram. The gradient complex amplitude statistics of the cell were determined using Fourier analysis of interferograms. From this complex information, 6 features were extracted. The differentiation of cells occurs through gradient stages. The author did not pay attention to the classification of stages and types.

Anand et al. (2012), suggests using digital holographic interference microscopy (DHIM) and numerical methods to automatically identify red blood cells infected with malaria. It is recognized by comparing its shape with healthy red blood cells. To distinguish between healthy and diseased cells, the correlation function is applied.

Lee & Lu (2011), reported that healthy RBCs and malaria-infected RBCs exhibit different spectra in elastic light scattering forward and backward directions. The backscatter of undiluted samples is a potential tool for non-invasive malaria diagnosis.

Gonzalez et al. (2015), suggested a system for evaluating the morphology of RBC in sickle cell anaemia samples that employs ellipse correction and algorithms to find noteworthy points. A system for effectively recognizing convex or concave points of interest in a contour is also included.

Xiong et al. (2010), proposed a consolidated area classification algorithm and quantified the distribution and accumulation of cells from the perspective of individual populations. It gives the measure of Goodness of Working Areas (GWA). This method combines erosion-based method and watershed technique to break up clumped cells.

This paper is organized as follows: Introduction to Malaria and its diagnosis is given in section 1. Section 2 gives review of literature. Methodology along with Systematically Applied Mean Filter and finding the 4-stage algorithm to get maximum accuracy with low computational complexity are described in section 3. Section 4 presents the system tests and results obtained. Section 5 validates precise malaria diagnosis systems by comparing it with existing method based on accuracy and finally conclusions are drawn in section 6.

2 Materials and Methods

Figure 2. Illustrates the proposed precise malaria diagnosis system which is made up of five major blocks for analyzing microscopic images.

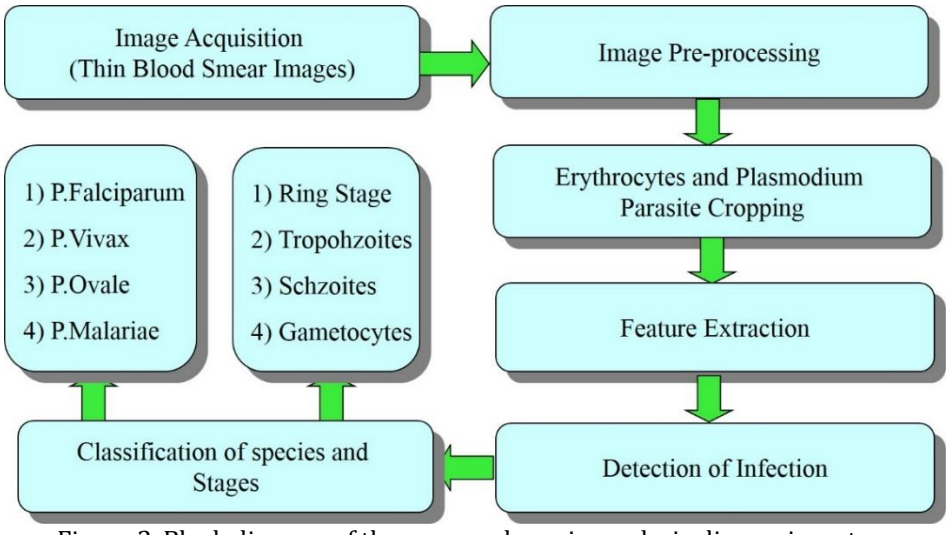

Figure 2. Block diagram of the proposed precise malaria diagnosis system

Image acquisition

Most malaria screening studies focus on thin images of blood smears; therefore, few studies use thick blood smear images. The image is usually taken using a charge-coupled device camera (CCD) coupled to the microscope. In this study, blood smear images, freely available on the Disease Control and Prevention (CDC), United States website were used.

Pre-processing

Complete diagnosis depends on image quality; therefore, any decrease in image quality can lead to poor disease diagnosis. Images are damaged mainly due to the noise that often occurs in the image acquisition stage. The commonly encountered noise in microscopic images is in the form of randomly spread black and white dots, called Salt & Pepper noise or impulse noise. In the presence of such corruption, it is difficult to identify the elements of the real image or to distinguish the infected area. A Systematically Applied Mean Filter (SAMF) is suggested in paper. This filter removes the impulse noise. The SAMF filter has been examined over highly corrupted malaria-infected blood images. The comparative results in indicate a notable improvement in image quality especially for high densities of noise.

Erythrocytes and plasmodium parasite cropping

The vital step in image processing and computer vision is segmentation. It is a procedure of dividing an image into a series of separate non-overlapping areas, which collectively form the entire image. The most important and difficult phase is to accurately isolate the blood smear image into red blood cells, white blood cells, plasmodium, etc. The segmentation of parasites and normal erythrocytes from the background is determined by the grouping of blood cells (infected and non-infected) in the image. Correct segmentation may effectively detect and classify malaria parasites. The review found that most researchers are using Otsu's algorithm to segment erythrocytes and malaria parasites. Several blood cell segmentation strategies have been proposed in recent studies. Table 2. summarizes the different segmentation approaches utilized by different studies.

Table 2
Techniques for segmentation

Reference papers	Techniques for Segmentation
Devi et al. [4], Lorenzo-Ginori et al. [40], Hartati et al. [41], Varma et al. [42], Mas et al. [8], Arco et al. [9], Tsai et al. [16], Hung et al. [17], Gosh et al. [19], Tomari et al. [10], Lee et al. [2], Ross et al. [27]	Otsu Thresholding.
Nag et al. [43], Sadiq et al. [44]	K-means clustering algorithm
Sadiq et al. [44]	Canny edge detection.
Pragya et al. [45], Purwar et al. [24]	Chanvese algorithm.
Tek et al. [12], Sio et al. [13]	Morphological Top Hat method.
Manning et al. [46], Kanojia et al. [47], Devi et al. [48], Buggenthin et al. [22]	Otsu followed by Watershed segmentation.

From above survey, in this study we used 6 algorithms for cropping blood cells from smear images as:

- Canny Edge Detector Algorithm;
- Chanvese;
- K-Means Clustering;
- Otsu;
- Otsu Followed by Watershed;
- Morphological Top Hat.

Features extraction

This is a big step towards the processing of most images for computer vision solutions, as it symbolizes the changeover from image to numerical data presentation. Other stain components and parasites are flexible objects of varying sizes and shapes. Color data is significant, but not enough to discriminate objects of different colors from different types of malaria parasites. A group of features that distinguish between normal features and infected cells is called a feature set. Many studies have found the texture and geometric characteristics to describe different stages of malaria. The different features used by researchers are summarized in table 3.

Table 3
Various Features used by different researchers in various studies

References	Features set
Devi et al. [4], Hartati et al. [41], Sadiq et al. [44], Kanojia et al. [47], Devi et al. [50]	Gray Level Co-occurrence Matrix (GLCM).
Devi et al. [4], Madhu G. [51], Sadiq et al. [44], Kanojia et al. [47], Tomari et al. [10], Das D.K. [11]	Hu moments.
Devi et al. [4], Sadiq et al. [44], Devi et al. [50], Das D.K. [11]	Linear Binary Pattern (LBP).
Nag et al. [43], Pragya et al. [45], Manning et al. [46], Hartati et al. [41], Kanojia et al. [47], Ghosh et al. [52], Delahunt et al. [20], Tomari et al. [10], Lee et al. [2], Das et al. [11], Tek et al. [12], Ross N. E. [27]	Shape Features.
Nag et al. [43], Lorenzo-Ginori et al. [40], Pragya et al. [45], Manning et al. [46], Kanojia et al. [47], Devi et al. [48], Ghosh et al. [52], Delahunt et al. [20], Lee et al. [2], Tek et al. [12], Ross N. E. [27]	Texture and Colour Descriptors.

Using image segmentation, blood cells were cropped and following features were extracted:

- Texture and Color – 17 Features
  3 Kurtosis of RGB, 3 Kurtosis of HSV, 3 Skewness of RGB, mean of RGB, mean of HSV, Average gray level, Standard deviation, Smoothness, Third moment, Uniformity and Entropy.
- Shape – 16 Features
  Form factor, Roundness, Aspect ratio, Compactness, mean area, mean eccentricity, mean Euler number, mean extent, mean perimeter, mean convex area, mean filled area, mean solidity, mean major axis, mean minor axis, mean diameter and N (no. of connected objects).
- GLCM – 4 features
  Contrast, correlation, energy and Homogeneity
- Hu moments – 7 features
  7 values that are invariant to object scale, position and orientation
- LBP – 59 features.

Classification

A decent feature extraction and segmentation procedure significantly simplify the development of classification. The classification procedure in automatic malaria diagnosis is usually used for two reasons: to determine erythrocyte infection and to classify the phase and type of malaria parasite. Table 3.3 includes the several classifiers that have been employed by different studies to classify infected cells, life stages, and species.

Table 4
Classification techniques used to classify infected erythrocytes

Reference papers	Techniques of Classification
Madhu G. [51]	Decision Tree
Nag et al. [43], Lorenzo-Ginori et al. [40], Das D. K. [11]	Naive Bayes
Kaur et al. [53], Nag et al. [43], Lorenzo-Ginori et al. [40], Pragya et al. [45], Hartati et al. [41], Gezahegn et al. [6], Sadiq et al. [44], Devi et al. [48], Das D. K. [11], Nanoti et al. [54].	Support Vector Machine.
Lorenzo-Ginori et al. [40], Devi et al. [48], Teket al. [12], Nanoti et al. [54], Devi et al. [50], Malihi et al. [55].	K Nearest Neighbour
Sadiq et al. [44]	Boosted Tree
Lorenzo-Ginori et al. [40], Ghosh et al. [52]	Bagged Tree
Devi et al. [4], Manning et al. [46], Kanojiaet al. [47], Devi et al. [48], Tomari et al. [10], Lee et al. [2], Ross N. E. [27], Gitonga et al. [56], Memeu D. M. [57] Memeu et al. [58].	Artificial Neural Network.

In this study we compared results of 13 classifiers and select the classifier which gives best accuracy. Following is the list of 13 classifiers:

- Fine Tree.
- Medium Tree.
- Coarse Tree.
- Kernel Naive Bayes.
- Linear Support Vector Machine.
- Quadratic Support Vector Machine.
- Cubic Support Vector Machine.
- Fine K Nearest Neighbour.
- Medium K Nearest Neighbour.
- Coarse K Nearest Neighbour.
- Ensemble Boosted Tree.
- Ensemble Bagged Tree.
- Artificial Neural Network.

3 Results and Discussions

Experimentation has been done the standard database available at Centre for Disease Control and Prevention (CDC), United States. The experiments were conducted with the help of Intel 7th generation i5-7200 central processing unit, having clock speed of 2.50 GHz and 8GB DDR4 RAM using MATLAB R2018a environment. Here we calculated accuracy and computational time complexity of overall system. CDC database has 17 response classes (16 infected and 1 non-infected). We had selected SAMF as a filter to remove impulse noise in pre-processing stage. We had taken various combinations of 6 cropping algorithms mentioned in section 3.3, 5 feature sets mentioned in section 3.4 and 13 classification algorithms mentioned in section 3.5, to get a combination of 4 stage system that gives highest accuracy. For classification we used 5-fold cross validation method. Table 4.1 gives the value of Accuracy for above mentioned combinations.

Table 5
Accuracy for SAMF, 6 cropping algorithms, 5 Feature extraction methods and 13 classifiers

Cropping Algorithms	Features	Accuracy for different classifiers												
		1	2	3	4	5	6	7	8	9	10	11	12	13
Canny Edge Detector	GLCM	84	82.3	80.9	74.8	78.4	84.2	72.2	93.4	84	80.8	84	89.6	80.4
	Hu_Moment	79.3	79.7	80	65.3	80.2	80.1	35	83	80.2	80.2	80.8	82.9	80.3
	LBP	76.9	81	82.1	42.2	82.9	83.5	82.5	71.6	79.8	81.6	82.4	83.3	82.7
	Shape	77.5	81	80.3	60	80.2	81.6	80.6	78.4	80.9	80.2	81.4	82.3	81.6
	Texture+Colour	88.5	85.6	83.8	72.7	88	93.1	94.1	95	85.7	80.6	87.6	93.8	87.1
Chanvese	GLCM	84.7	85	85.2	81	85.6	87	73.6	93.5	85.6	84.4	86.2	90.2	84.6
	Hu_Moment	83.2	84.4	84.2	63	84.5	61.1	15.4	91.7	83.6	84.4	85.5	86.3	84.4
	LBP	78.9	83	83.2	57.4	86.3	86.2	86	76.2	84.2	84.4	86	86.2	86.8
	Shape	90.1	88.3	85.6	82.7	89.9	93.6	93.7	95	88.1	84.4	91.5	94.6	84.6
	Texture+Colour	90.9	88.6	85.4	82.2	89.7	93.7	94.2	95.1	55.4	84.4	91.8	95.1	88.5
K-Means Clustering	GLCM	84.3	83.1	81.6	75.6	82	86	76.9	93.1	85	82.4	84.1	90.2	84.1
	Hu_Moment	80.6	81.4	81.8	61.4	81.8	52.3	6.2	87	81.2	81.8	81.9	83.6	81.8
	LBP	78.1	82.8	83.5	33.9	83.9	84.1	83.2	71.1	81.3	82.6	83.7	84.3	83.4
	Shape	81.9	83.4	82.6	68.2	82.3	84.6	84.7	82.4	82.6	82.3	83.7	86.4	82.9
	Texture+Colour	89.3	87.1	85.4	70.5	87.9	93.4	94.3	93.8	86.9	82.3	88	94	85.7
Otsu	GLCM	87.7	86.4	85.5	78.3	85.7	89	65.8	94.9	88.6	86.3	87.3	92.6	86
	Hu_Moment	84.8	85.3	85.6	64.1	85.6	25.4	7	89.9	85.6	85.6	85.7	86.8	85.6
	LBP	84.2	86.4	86.8	41.7	87.3	88	87.4	74.1	83.4	87	87.1	87.6	86.9
	Shape	87.4	87.6	86.2	75.4	87.4	89.3	89	87.2	88	86.8	87.9	89.9	87.5
	Texture+Colour	91.8	90	88.6	74.6	90.9	95.6	96.5	96.4	90.7	86.5	91.1	96.4	90.4
Otsu Followed by Watershed	GLCM	88.2	88.2	87.6	83.1	87.6	88.8	18.5	88.3	88.6	87.8	88.3	89.8	87.9
	Hu_Moment	86.5	87.2	87.1	77.8	87.1	14	2.6	82.1	87.1	87.1	87.3	87.7	87.1
	LBP	86.9	87.7	87.2	68	88.5	88.9	88.6	80.1	87.5	88.1	88.4	88.5	88.6
	Shape	87.1	87.3	87.1	73.5	87.8	88.3	88.7	85.3	87.8	87.5	87.6	89	87.5
	Texture+Colour	91.2	89.9	88.5	76	91.9	94.9	95.6	94.8	92.3	89	90.5	94.1	90.5
Morphological Top Hat	GLCM	73	72.9	70.3	63.2	70.7	76.1	71.8	87	74.1	71.7	74.1	82.5	70.9
	Hu_Moment	69.2	70.6	70.1	60.4	70.7	69.8	40.2	71.9	69.9	70.7	71.2	73.4	68.4
	LBP	66.1	72.4	72.7	18.2	73.5	73.9	72	56.8	71.3	72.1	72.8	73.3	72
	Shape	68.6	72	71.7	60.9	70.8	73.5	72.7	67.6	71.1	71.6	73	75.7	69.2
	Texture+Colour	79.6	75.9	74.9	51.4	77	84.7	86.1	87.8	76.4	71.1	77.1	87.5	71.8

From above table 5, we can write the summary table 4.2 for CDC dataset which gives us the combination of 4 stage system with highest accuracy and less time complexity.

Table 6
Summary for CDC dataset to get 4 stage system with highest accuracy and less time complexity

Filter	Segmentation	Feature	Classifier	Accuracy	Filter+ Cropping Time	Feature Extraction Time	Prediction time	Total time required for predicting one image
				(%)	(sec)	(sec)	(sec)	(sec)
SAMF	Canny edge detector	Texture+Colour	Fine KNN	95	0.438541	0.0034904	0.0007565	0.442788
SAMF	Chanvese	Texture+Colour	Fine KNN	95.1	11.995889	0.0100713	0.0005372	12.006498
SAMF	Kmean	Texture+Colour	Cubic SVM	94.3	4.5762395	0.0046828	0.0050246	4.585947
SAMF	Otsu	Texture+Colour	Cubic SVM	96.5	0.4263418	0.0044274	0.0069430	0.437712
SAMF	Otsu+WSS	Texture+Colour	Cubic SVM	95.6	0.4550498	0.0035140	0.0095783	0.4681423
SAMF	Top Hat	Texture+Colour	Fine KNN	87.8	0.5244139	0.0036875	0.0007467	0.5288483

From above summary, for CDC database, the combination of 4 stage system which give highest accuracy of 96.50% with time required to predict one sample as 0.437712sec consist of: SAMF as filter, Otsu algorithm for erythrocytes and parasite cropping, 17 texture and color feature set and cubic SVM as classifier.

System Design and Validation

So, from table 6 we can draw conclusion that, to design precise malaria diagnosis system, we need to choose SAMF as filter, Otsu algorithm for erythrocytes and parasite cropping, 17 texture and color feature set and cubic SVM as classifier.
The final block diagram of the precise malaria diagnosis system is shown in figure 3.

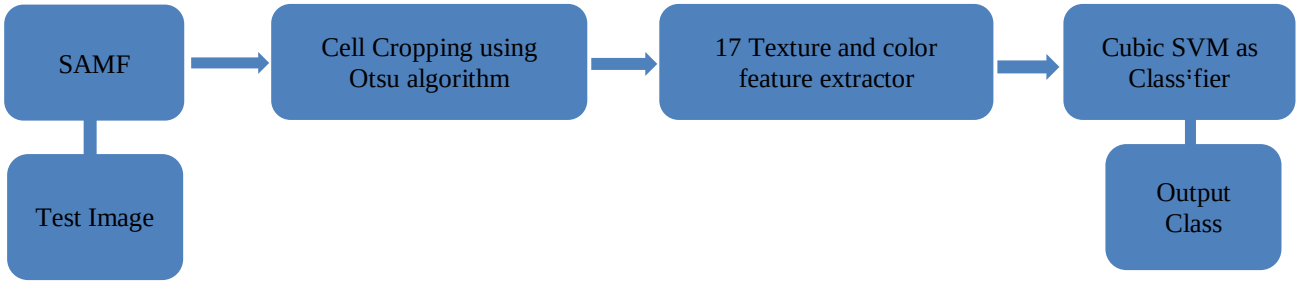

Figure 3. Block diagram of precise malaria diagnosis system

We have validated our precise malaria diagnosis systems by comparing it with existing method based on accuracy. For validation, we have used 5-fold cross validation technique on CDC database.

Table 7
Sensitivity/Recall, Specificity, Precision, F1-score and Accuracy for each class as well as their average values.

Class	TP	TN	FP	FN	Sensitivity/ Recall (%)	Specificity (%)	Precision (%)	F1-score (%)	Accuracy (%)
F1	187	4764	26	22	89.47	99.46	87.79	88.63	99.04
F2	60	4912	12	15	80.00	99.76	83.33	81.63	99.46
F3	48	4922	6	23	67.61	99.88	88.89	76.80	99.42
F4	19	4979	0	1	95.00	100.00	100.00	97.44	99.98
M1	11	4987	0	1	91.67	100.00	100.00	95.65	99.98
M2	27	4946	13	13	67.50	99.74	67.50	67.50	99.48
M3	14	4980	3	2	87.50	99.94	82.35	84.85	99.90
M4	33	4955	1	10	76.74	99.98	97.06	85.71	99.78
O1	18	4969	3	9	66.67	99.94	85.71	75.00	99.76
O2	26	4963	1	9	74.29	99.98	96.30	83.87	99.80
O3	19	4978	1	1	95.00	99.98	95.00	95.00	99.96
O4	20	4971	1	7	74.07	99.98	95.24	83.33	99.84
V1	46	4925	14	14	76.67	99.72	76.67	76.67	99.44
V2	6	4991	0	2	75.00	100.00	100.00	85.71	99.96
V3	26	4959	7	7	78.79	99.86	78.79	78.79	99.72
V4	21	4974	2	2	91.30	99.96	91.30	91.30	99.92
NI	4241	632	87	39	99.09	87.90	97.99	98.54	97.48
		Average			**81.55**	**99.18**	**89.64**	**85.08**	**99.58**

Where,
F1: Ring-form trophozoites of P. falciparum.
F2: Older trophozoites of P. falciparum.
F3: Gametocytes of P. falciparum.
F4: Schizonts of P. falciparum.
M1: Ring-form trophozoites of P. malariae.
M2: Older trophozoites of P. malariae.
M3: Gametocytes of P. malariae.
M4: Schizonts of P. malariae.
O1: Ring-form trophozoites of P. ovale
O2: Older trophozoites of P. ovale.
O3: Gametocytes of P. ovale.
O4: Schizonts of P. ovale.
V1: Ring-form trophozoites of P. vivax.
V2: Older trophozoites of P. vivax.
V3: Gametocytes of P. vivax.
V4: Schizonts of P. vivax

Also, Overall accuracy can be calculated from total true positive (TTP), total true negative (TTN), total false positive (TFP) and total false negative (TFN). These values are calculated from confusion matrix of 17 classes and have values as:

TTP = 581 TTN = 4241 TFP = 105 TFN = 72

Therefore,

$$Overall\ Accuracy = \frac{TTP + TTN}{TTP + TTN + TFP + TFN}$$

$$Overall\ Accuracy = \frac{581 + 4241}{581 + 4241 + 107 + 72} = 0.965$$

$$\% \, \boldsymbol{Overall\ Accuracy} = \mathbf{96.50}\%$$

Following table 8 give the validation of precise malaria diagnosis systems with existing methods.

Table 8
Validation of precise malaria diagnosis systems with existing methods

Ref. No.	Title	Year	Accuracy
12	"Malaria Detection and Classification Using Machine Learning Algorithms" [12]	2018	78.89%
14	"Automatic Identification of Malaria Using Image Processing and Artificial Neural Network" [2]	2018	78.00%
16	"Automatic System for Plasmodium Species Identification from Microscopic Images of Blood-Smear Samples" [15]	2017	72.73% (from confusion matrix)
43	"Detection and Classification of Malaria in Thin Blood Slide Images" [44]	2017	94.97%
44	"Detection of malaria parasite species and life cycle stages using microscopic images of thin blood smear" [45]	2016	90.17%
45	"kNN Classification based Erythrocyte Separation in Microscopic Images of Thin Blood Smear" [46]	2016	94.20%
46	"Determination of Plasmodium Parasite Life Stages and Species in Images of Thin Blood Smears Using Artificial Neural Network" [47]	2014	Stages Accuracy: 90.34% Species Accuracy: 95.85%
47	"A Rapid Malaria Diagnostic Method Based on Automatic Detection and Classification of Plasmodium Parasites in Stained Thin Blood Smear Images" [48]	2014	Stages Accuracy: 90.34% Species Accuracy: 95.85%
48	"Malaria Parasite Detection in Giemsa–Stained Blood Cell Images" [49]	2013	91%
49	"Detection of plasmodium parasites from images of thin blood smears" [50]	2013	95.00%
50	"Blood Parasite Identification using Feature Based Recognition" [51]	2011	68.96%
51	"An Image Processing Approach for Accurate Determination of Parasitemia in Peripheral Blood Smear Images" [52]	2011	From confusion matrix 96.05%
52	"An Efficient Algorithm for Automatic Malaria Detection in Microscopic Blood Images" [53]	2012	From confusion matrix 96.05%
	Design of precise malaria diagnosis system using microscopic imaging.	2022	Average Accuracy: 99.58% Overall Accuracy: 96.5%

From above analysis we can say that the precise malaria diagnosis system gives an Average accuracy of 99.58% and Overall accuracy of 96.5% which is greater than the accuracy obtained for CDC database by existing methods listed in table 5.2.

4 Conclusion

In SAMF algorithm is proposed that removes impulse noise from the corrupted malaria-infected images. The suggested SAMF can be used as a reliable pre-processing method for disease detection in microscopic medical images. Otsu method is used to obtain the binary version of images for cropping blood cells from complete image. 17 texture and color features were extracted from these cropped cells and these features were used to train Cubic SVM classifier. Hence, using images of thin blood smears, a precise malaria diagnosis system was developed for detecting Plasmodium parasites, distinguishing their life stages, and species. To train and test the system, a total of 348 images from the CDC database were used. In recognizing the presence of Plasmodium parasites in thin blood smear images, the system had an average accuracy of 99.58% and an overall accuracy of 96.5% with prediction time of 0.437712sec/sample. Also, we have validated the results by comparing with existing methods. Patients in rural areas can be benefited from a precise malaria diagnosis method. When compared to the manual microscopic diagnosis technique, the proposed technology detects malaria parasites faster.

Acknowledgments
This research was supported by Sandip Institute of Technology and Research Center, Nashik, MS, India.

References

Anand, A., Chhaniwal, V. K., Patel, N. R., & Javidi, B. (2012). Automatic identification of malaria-infected RBC with digital holographic microscopy using correlation algorithms. *IEEE Photonics Journal*, *4*(5), 1456-1464.

Arco, J. E., Górriz, J. M., Ramírez, J., Álvarez, I., & Puntonet, C. G. (2015). Digital image analysis for automatic enumeration of malaria parasites using morphological operations. *Expert Systems with Applications*, *42*(6), 3041-3047. https://doi.org/10.1016/j.eswa.2014.11.037

Banoth, E., Jagannadh, V. K., & Gorthi, S. S. (2015). Single-cell optical absorbance characterization with high-throughput microfluidic microscopy. *IEEE Journal of Selected Topics in Quantum Electronics*, *22*(3), 111-116.

Buggenthin, F., Marr, C., Schwarzfischer, M., Hoppe, P. S., Hilsenbeck, O., Schroeder, T., & Theis, F. J. (2013). An automatic method for robust and fast cell detection in bright field images from high-throughput microscopy. *BMC bioinformatics*, *14*(1), 1-12.

Campuzano-Zuluaga, G., Hänscheid, T., & Grobusch, M. P. (2010). Automated haematology analysis to diagnose malaria. *Malaria Journal*, *9*(1), 1-15.

Center of Disease Controal and Prevention. (n.d.). (U.S. Department of Health & Human Services) Retrieved August 2020, from https://www.cdc.gov/dpdx/malaria/index.html

Chen, H. M., Tsao, Y. T., & Tsai, S. N. (2014). Automatic image segmentation and classification based on direction texton technique for hemolytic anemia in thin blood smears. *Machine vision and applications*, *25*(2), 501-510.

Das, D. K., Ghosh, M., Pal, M., Maiti, A. K., & Chakraborty, C. (2013). Machine learning approach for automated screening of malaria parasite using light microscopic images. *Micron*, *45*, 97-106. https://doi.org/10.1016/j.micron.2012.11.002

Delahunt, C., Horning, M. P., Wilson, B. K., Proctor, J. L., & Hegg, M. C. (2014). Limitations of haemozoin-based diagnosis of Plasmodium falciparum using dark-field microscopy. *Malaria journal*, *13*(1), 1-10.

Devi, S. S., Laskar, R. H., & Sheikh, S. A. (2018). Hybrid classifier based life cycle stages analysis for malaria-infected erythrocyte using thin blood smear images. *Neural Computing and Applications*, *29*(8), 217-235.

Elsalamony, H. A. (2016). Healthy and unhealthy red blood cell detection in human blood smears using neural networks. *Micron*, *83*, 32-41. https://doi.org/10.1016/j.micron.2016.01.008

Eluru, G., Srinivasan, R., & Gorthi, S. S. (2015). Deformability Measurement of Single-Cells at High-Throughput With Imaging Flow Cytometry. *Journal of Lightwave Technology*, *33*(16), 3475-3480.

Fatima, T., & Farid, M. S. (2020). Automatic detection of Plasmodium parasites from microscopic blood images. *Journal of Parasitic Diseases*, *44*(1), 69-78.

Gezahegn, Y. G., Medhin, Y. G., Etsub, E. A., & Tekele, G. G. (2018). Malaria Detection and Classification. ICT4DA 2017, LNICST 244, Springer, 24-33.

Ghosh, P., Bhattacharjee, D., & Nasipuri, M. (2017). Automatic system for plasmodium species identification from microscopic images of blood-smear samples. *Journal of Healthcare Informatics Research*, *1*(2), 231-259.

Gonzalez-Hidalgo, M., Guerrero-Pena, F. A., Herold-García, S., Jaume-i-Capó, A., & Marrero-Fernández, P. D. (2014). Red blood cell cluster separation from digital images for use in sickle cell disease. *IEEE journal of biomedical and health informatics*, *19*(4), 1514-1525.

Hartati, S., Harjoko, A., Rosnelly, R., & Chandradewi, I. (2018, August). Performance of SVM and ANFIS for classification of malaria parasite and its life-cycle-stages in blood smear. In *International Conference on Soft Computing in Data Science* (pp. 110-121). Springer, Singapore.

Hung, Y. W., Wang, C. L., Wang, C. M., Chan, Y. K., Tseng, L. Y., Lee, C. W., & Tung, K. C. (2015). Parasite and infected-erythrocyte image segmentation in stained blood smears. *Journal of Medical and Biological Engineering*, *35*(6), 803-815.

Kanojia, M., Gandhi, N., Armstrong, L. J., & Pednekar, P. (2017, December). Automatic identification of malaria using image processing and artificial neural network. In *International Conference on Intelligent Systems Design and Applications* (pp. 846-857). Springer, Cham.

Kaur, D., & Walia, G. K. (2020). A hybrid aco-svm approach for detecting and classifying malaria parasites. In *Computational Network Application Tools for Performance Management* (pp. 139-152). Springer, Singapore.

Khanna, P., & Kumar, S. (2020). Malaria parasite classification employing chan–vese algorithm and SVM for healthcare. In *Proceedings of First International Conference on Computing, Communications, and Cyber-Security (IC4S 2019)* (pp. 697-711). Springer, Singapore.

Khashman, A. (2008). IBCIS: Intelligent blood cell identification system. *Progress in Natural Science*, *18*(10), 1309-1314. https://doi.org/10.1016/j.pnsc.2008.03.026

Lee, H., & Chen, Y. P. P. (2014). Cell morphology based classification for red cells in blood smear images. *Pattern Recognition Letters*, *49*, 155-161. https://doi.org/10.1016/j.patrec.2014.06.010

Lee, S., & Lu, W. (2011). Using elastic light scattering of red blood cells to detect infection of malaria parasite. *IEEE transactions on biomedical engineering*, *59*(1), 150-155.

Lorenzo-Ginori, J. V., Chinea-Valdés, L., Izquierdo-Torres, Y., Orozco-Morales, R., Mollineda-Diogo, N., Sifontes-Rodríguez, S., & Meneses-Marcel, A. (2019, October). Classification of Plasmodium-Infected Erythrocytes Through Digital Image Processing. In *Latin American Conference on Biomedical Engineering* (pp. 351-360). Springer, Cham.

Madhu, G. (2020). Computer vision and machine learning approach for malaria diagnosis in thin blood smears from microscopic blood images. In *Machine learning for intelligent decision science* (pp. 191-209). Springer, Singapore.

Malihi, L., Ansari-Asl, K., & Behbahani, A. (2013, September). Malaria parasite detection in giemsa-stained blood cell images. In *2013 8th Iranian conference on machine vision and image processing (MVIP)* (pp. 360-365). IEEE.

Manning, K., Zhai, X., & Yu, W. (2019). Image Analysis Based System for Assessing Malaria. In *Cyberspace Data and Intelligence, and Cyber-Living, Syndrome, and Health* (pp. 466-486). Springer, Singapore.

Mas, D., Ferrer, B., Cojoc, D., Finaurini, S., Mico, V., Garcia, J., & Zalevsky, Z. (2015). Novel image processing approach to detect malaria. *Optics Communications*, *350*, 13-18.https://doi.org/10.1016/j.optcom.2015.03.064

Memeu, D. M. (2014). *A rapid malaria diagnostic method based on automatic detection and classification of plasmodium parasites in stained thin blood smear images* (Doctoral dissertation, University of Nairobi).

Moon, I., Anand, A., Cruz, M., & Javidi, B. (2013). Identification of malaria-infected red blood cells via digital shearing interferometry and statistical inference. *IEEE Photonics Journal*, *5*(5), 6900207-6900207.

Nag, S., Basu, N., & Bandyopadhyay, S. K. (2020). Application of machine intelligence in digital pathology: Identification of falciparum malaria in thin blood smear image. In *Advancement of machine intelligence in interactive medical image analysis* (pp. 65-97). Springer, Singapore.

Nanoti, A., Jain, S., Gupta, C., & Vyas, G. (2016, August). Detection of malaria parasite species and life cycle stages using microscopic images of thin blood smear. In *2016 International Conference on Inventive Computation Technologies (ICICT)* (Vol. 1, pp. 1-6). IEEE.

Nixon, M. (2008). Feature extraction & image processing. Cambridge: Academic press.

Okhabska, I., Budzyn, V., Rybchych, I., Zyma, I., & Kalichak, Y. (2022). Management of medical institutions on context of provision medical and preventive care in COVID-19 condition. International Journal of Health Sciences, 6(1), 347-356. https://doi.org/10.53730/ijhs.v6n1.4381

Omucheni, D. L., Kaduki, K. A., Bulimo, W. D., & Angeyo, H. K. (2014). Application of principal component analysis to multispectral-multimodal optical image analysis for malaria diagnostics. *Malaria journal*, *13*(1), 1-11.

Prasad, K., Winter, J., Bhat, U. M., Acharya, R. V., & Prabhu, G. K. (2012). Image analysis approach for development of a decision support system for detection of malaria parasites in thin blood smear images. *Journal of digital imaging*, *25*(4), 542-549.

Purwar, Y., Shah, S. L., Clarke, G., Almugairi, A., & Muehlenbachs, A. (2011). Automated and unsupervised detection of malarial parasites in microscopic images. *Malaria journal*, *10*(1), 1-11.

Rakshit, P., & Bhowmik, K. (2013). Detection of presence of parasites in human RBC in case of diagnosing malaria using image processing. In *2013 IEEE Second International Conference on Image Information Processing (ICIIP-2013)* (pp. 329-334). IEEE.

Ross, N. E., Pritchard, C. J., Rubin, D. M., & Duse, A. G. (2006). Automated image processing method for the diagnosis and classification of malaria on thin blood smears. *Medical and Biological Engineering and Computing*, *44*(5), 427-436.

Sadiq, M. J., & Balaram, V. V. S. S. S. (2018). OFS-Z: Optimal Features Selection by Z-Score for Malaria-Infected Erythrocyte Detection Using Supervised. In *Proceedings of the Second International Conference on Computational Intelligence and Informatics: ICCII 2017* (Vol. 712, p. 221). Springer.

Sio, S. W., Sun, W., Kumar, S., Bin, W. Z., Tan, S. S., Ong, S. H., ... & Tan, K. S. (2007). MalariaCount: an image analysis-based program for the accurate determination of parasitemia. *Journal of microbiological methods*, *68*(1), 11-18. https://doi.org/10.1016/j.mimet.2006.05.017

Somasekar, J., & Reddy, B. E. (2015). Segmentation of erythrocytes infected with malaria parasites for the diagnosis using microscopy imaging. *Computers & Electrical Engineering*, *45*, 336-351. https://doi.org/10.1016/j.compeleceng.2015.04.009

Srivastava, B., Anvikar, A. R., Ghosh, S. K., Mishra, N., Kumar, N., Houri-Yafin, A., ... & Valecha, N. (2015). Computer-vision-based technology for fast, accurate and cost effective diagnosis of malaria. *Malaria journal*, *14*(1), 1-6.

Tek, F. B., Dempster, A. G., & Kale, I. (2009). Computer vision for microscopy diagnosis of malaria. *Malaria journal*, *8*(1), 1-14.

Tek, F. B., Dempster, A. G., & Kale, I. (2010). Parasite detection and identification for automated thin blood film malaria diagnosis. *Computer vision and image understanding*, *114*(1), 21-32. https://doi.org/10.1016/j.cviu.2009.08.003

Tomari, R., Zakaria, W. N. W., Jamil, M. M. A., Nor, F. M., & Fuad, N. F. N. (2014). Computer aided system for red blood cell classification in blood smear image. *Procedia Computer Science*, *42*, 206-213. https://doi.org/10.1016/j.procs.2014.11.053

Tsai, M. H., Yu, S. S., Chan, Y. K., & Jen, C. C. (2015). Blood smear image based malaria parasite and infected-erythrocyte detection and segmentation. *Journal of medical systems*, *39*(10), 1-14.

Varma, S. L., & Chavan, S. S. (2019). Detection of malaria parasite based on thick and thin blood smear images using local binary pattern. In *Computing, Communication and Signal Processing* (pp. 967-975). Springer, Singapore.

World Malaria Report. (2019). Switzerland.: World Health Organization http://www.who.int/malaria.

Xiong, W., Ong, S. H., Lim, J. H., Foong, K. W. C., Liu, J., Racoceanu, D., ... & Tan, K. S. (2010). Automatic area classification in peripheral blood smears. *IEEE Transactions on Biomedical Engineering*, *57*(8), 1982-1990.

Biography of Authors

Mosam K. Sangole
Received his M.Tech. Degree in Electronics from College of Engineering, Pune, India. Currently, he is pursuing PhD degree from the Savitribai Phule Pune University. He is working as a researcher at Research Lab since 2016. His research interests include image and video processing, medical image analysis, and diagnosis of malaria parasite from microscopic blood smear images.
Email: mosamleo@gmail.com

Dr. Sanjay T. Gandhe
Is Principal of Sandip Institute of Technology & Research Centre, Nashik. He completed B.E., M.E. and Ph.D. (VNIT, Nagpur) in 1990, 1996 and 2008 respectively. He has published 27 research papers in International Journals and presented 41 papers in National /International Conferences. He is fellow member of IETE, IEI, Senior Member of IEEE and life member of ISTE. He has fetched several Research Grants from Governmental Apex Bodies. He is honored as Best Principal Award and Best Teachers in Professional Educational Category. He was Reviewer of IEEE Transaction on Dependable and Secure Computing in 2011-12. He served as Session Chair in various National and International Conferences. His area of expertise is Image Processing, Robotics and Machine Vision.
Email: stgandhe@gmail.com